Bulletin of Electrical Engineering and Informatics
Vol. 15, No. 3, June 2026, pp. 2853~2872
ISSN: 2302-9285, DOI: 10.11591/eei.v15i3.11565

Comparative analysis of switching frequency in DTC-CBSVM and FOC of three-level NPC PMSM drive for EV applications

Rakesh Shriwastava[1,2], Balajee Maram[1], Yogesh S. Pawar[3], Jyoti P. Rothe[4], Dinesh S. Wankhede[4], Hema Kale[5]

[1]Department of Computer Science and Artificial Intelligence, SR University, Warangal, India
[2]Department of Electrical Engineering, Govindrao Wanjari College of Engineering and Technology, Nagpur, India
[3]Department of Electrical Engineering, Loknete Gopinathaji Munde Institute of Engineering Education and Research, Nashik, India
[4]Department of Electrical Engineering, St. Vincent Pallotti College of Engineering and Technology, Nagpur, India
[5]Department of Electronics and Telecommunication, St. Vincent Pallotti College of Engineering and Technology, Nagpur, India

Article Info

Article history:

Received Oct 8, 2025
Revised Apr 9, 2026
Accepted Apr 19, 2026

Keywords:

Carrier-based space vector modulation
Direct torque control
Permanent magnet synchronous motor
Torque harmonic distortion
Twelve-switch neutral point clamped (TS-NPC) inverter

ABSTRACT

This paper presents a comparative analysis of switching frequency performance in direct torque control with carrier-based space vector modulation (DTC-CBSVM) and field-oriented control (FOC) of permanent magnet synchronous motor (PMSM) drives fed by a three-level neutral point clamped (NPC) inverter. PMSM drives are widely utilized in electric vehicles (EVs) due to their high efficiency, torque density, and reliability. However, the selection of an appropriate control strategy significantly influences inverter switching frequency, system efficiency, and overall drive performance. The DTC-CBSVM approach provides fast torque response and reduced torque ripple, whereas the FOC technique ensures precise control of flux and torque with smoother operation. In this study, both methods are implemented and evaluated under identical operating conditions. Simulation results highlight the trade-offs between dynamic response, switching frequency, and harmonic performance. The findings serve as a reference for selecting optimal control strategies for efficient PMSM-based NPC inverter drives in EV applications.

Corresponding Author:

Rakesh Shriwastava
Department of Electrical Engineering, Govindrao Wanjari College of Engineering and Technology
Nagpur, India
Email: rakesh_shriwastava@rediffmail.com

1. INTRODUCTION

Permanent magnet synchronous motors (PMSMs) are rapidly becoming the preferred choice for electric vehicle (EV) propulsion systems, owing to their high power density, high efficiency, and excellent torque-to-inertia ratio [1], [2]. To realize these advantages, the motor drive and control strategy are critical, particularly the choice of inverter topology and control algorithm [3], [4]. Three-level neutral point clamped (NPC) inverters offer several benefits over traditional two-level inverters: lower voltage stress on power switching devices, reduced harmonic distortion in output voltage, improved voltage quality, and lower switching losses for a given DC link voltage [5], [6]. These features are especially important in high-power EV inverters, where efficiency, thermal stress, and reliability are all decisive [7], [8]. Among the various control schemes, field-oriented control (FOC) and direct torque control (DTC) are two leading contenders [9], [10]. FOC uses pulse width modulation (PWM) or space vector pulse width modulation (SVPWM) to generate voltage commands based on transformed d–q axis current references, delivering smooth torque, good steady-state performance, and predictable switching frequency [11], [12]. On the other hand, DTC,

especially when augmented with carrier-based space vector modulation (CBSVM), offers faster dynamic torque response, and a simpler control structure, but often at the cost of variable switching frequency and increased torque ripple [13], [14].

Switching frequency is an important design parameter in EV drives, as it impacts inverter switching losses, thermal loading, electromagnetic interference (EMI), acoustic noise, filter design, and the overall efficiency and reliability of the power electronics [15], [16]. Given that FOC tends to employ fixed or quasi-fixed switching frequency through PWM/SVPWM techniques, while DTC-CBSVM can lead to more variable switching behavior, a comparative study under identical operating conditions is essential to determine which control strategy better balances dynamic performance and efficiency in practical EV inverter designs [17], [18]. Several studies have highlighted the influence of switching frequency on harmonic distortion, inverter losses, and torque quality in PMSM drive systems [19], [20]. Moreover, the adoption of multilevel inverter topologies in EV applications has increased due to their capability to enhance power quality and reduce device stress [21], [22].

Therefore, this paper aims to perform a comparative analysis of switching frequency behavior between DTC-CBSVM and FOC control strategies for a PMSM powered through a three-level NPC inverter under various operating conditions relevant to EV applications, such as speed variations, load disturbances, and transient operating conditions [23], [24]. The analysis investigates not only the average switching frequency but also its variation and impact on torque ripple, harmonic distortion, switching losses, and overall drive efficiency to assist designers in selecting the optimal control strategy for EV drive applications [25].

This paper is organized as follows: section 1 presents the introduction. Section 2 describes the analysis and modeling of the PMSM. Section 3 explains the proposed method. Section 4 present the simulation and hardware results, respectively. Finally, section 5 concludes the paper.

2. PERMANENT MAGNET SYNCHRONOUS MOTOR MODEL ANALYSIS

The direct-axis winding induced voltage is given by:

$$u_d = R_d i_d + \frac{d\lambda_d}{dt} - \omega_r \lambda_q \quad (1)$$

In (1), R_d are the stator resistance and id are the stator current of direct-axis.
The quadrature-axis winding induced voltage is given by:

$$u_d = R_q i_q + \frac{d\lambda_d}{dt} - \omega_r \lambda_d \quad (2)$$

In (2), R_q are the stator resistance and i_q are the stator current of quadrature-axis:

$$\lambda_d = L_q i_q + \lambda_m \quad (3)$$

In (3), λ_d are the flux-linkage of stator direct-axis and λ_m is the rotor flux:

$$\lambda_q = L_q i_q \quad (4)$$

In (4), λ_q are the flux-linkage of stator quadrature -axis and λ_m is absent:

$$L_d = L_q \quad (5)$$

In (6), PMSM torque equation is:

$$T_e = \frac{3}{2}\frac{p}{2}(\lambda_d i_q - \lambda_q i_{d)} \quad (6)$$

Put the value of (3) and (4) in (6).

$$T_e = \frac{3}{2}\frac{p}{2}[(\lambda_d i_d + \lambda_m) i_q - L_q i_q i_d] \quad (7)$$

$$T_e = \frac{3}{2}\frac{p}{2}[\left(L_d - L_q\right) i_d i_q + \lambda_m i_q] \quad (8)$$

From (8) has two different components shown in (9) and (10):

$$Reluctance\ torque = \frac{3}{2}\frac{p}{2}\left(L_d - L_q\right)i_d i_q] \quad (9)$$

$$Field\ torque = \frac{3}{2}\frac{p}{2}\lambda_m i_q \quad (10)$$

Due to PM flux linkage, λ_m the electromagnetic torque is (6).

$$T_e = \frac{3}{2}\frac{p}{2}\lambda_m i_q \quad (11)$$

The constant parameters are rotor flux-linkage and number of poles in round-rotor PMSM.
The electromagnetic torque equation is:

$$T_e = Kt\ i_q \quad (12)$$

K_t is torque constant:

$$K_t = K\frac{3}{2}\frac{p}{2}\lambda_m$$

Therefore, mechanical torque is given by (13):

$$T_e = T_i + B\omega_m + J\frac{d\omega_m}{dt} \quad (13)$$

ω_m and ω_r are the rotor's mechanical and electrical speed.

3. PROPOSED METHOD

The proposed work focuses on the comparative analysis of switching frequency performance between direct torque control with carrier-based space vector modulation (DTC-CBSVM) and FOC of a PMSM fed by an NPC inverter for EV applications. The methodology consists of system modeling, implementation of control strategies, simulation environment, performance evaluation, and comparative analysis.

In system modeling, the mathematical model of a surface-mounted PMSM is developed in the d–q reference frame, including stator voltage equations, flux linkages, and electromagnetic torque equations. A three-level NPC inverter is also modeled with appropriate switching states and voltage vectors to interface with the PMSM.

In the implementation of the first control strategy, FOC employs Clarke and Park transformations to decouple torque and flux components. Reference currents for the d–q axes are generated using proportional–integral (PI) controllers, and SVPWM is used for gate pulse generation, ensuring fixed switching frequency operation.

In the implementation of the second control strategy, DTC-CBSVM estimates stator flux and torque using real-time voltage and current measurements. Hysteresis controllers are employed to regulate flux and torque within reference bands. Carrier-based SVM is used instead of conventional lookup tables to reduce torque ripple and achieve a quasi-constant switching frequency.

In the simulation environment, both control schemes are implemented in MATLAB/Simulink under identical operating conditions, such as constant speed, variable load torque, and transient acceleration. Identical PMSM and inverter parameters are applied to ensure a fair comparison.

For performance evaluation, switching frequency behavior, including mean value, variation range, and frequency spectrum, is measured. Dynamic torque response, total harmonic distortion (THD), inverter losses, and torque ripple are compared for both DTC-CBSVM and FOC. The impact of switching behavior on drive efficiency and suitability for EV applications is also assessed.

Finally, the comparative analysis examines the trade-offs between FOC, which offers fixed switching frequency and smoother operation but slower dynamic response, and DTC-CBSVM, which provides faster response and improved dynamic performance with quasi-constant switching frequency using CBSVM. Quantitative results are presented through tables, graphs, and time-domain waveforms for direct comparison. Figure 1 shows the block schematic of the proposed DTC-CBSVM method, while Figure 2 shows the block schematic of the proposed FOC-SVPWM method.

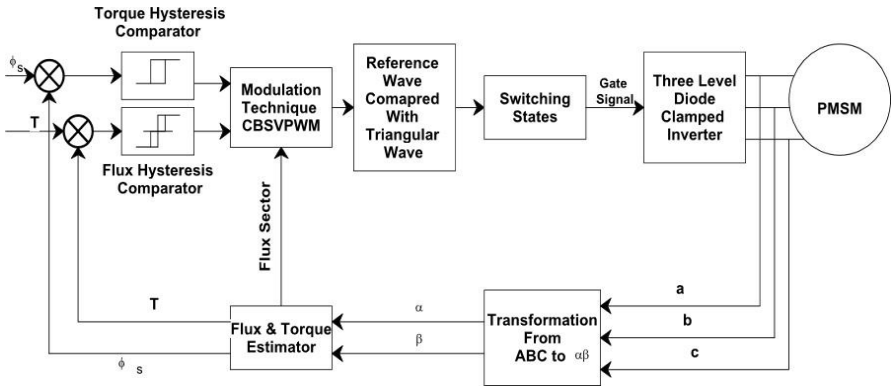

Figure 1. Block schematic of novel DTC–CBSVM

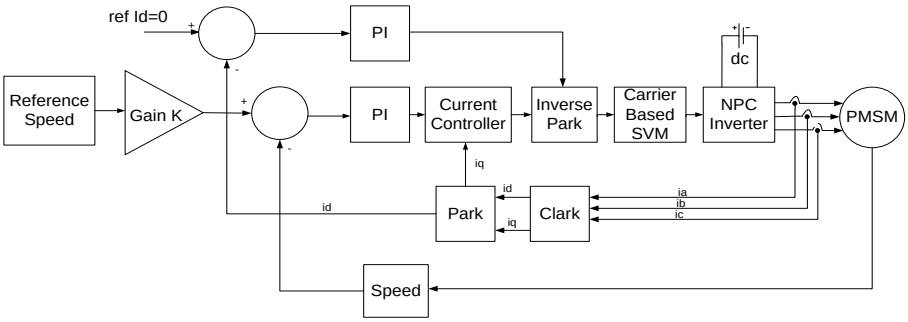

Figure 2. Block schematic of novel FOC-CBSVM

4. SIMULATIONS RESULTS ANALYSIS

DTC-CBSVM-based twelve-switch NPC inverter (NPCI) PMSM drive performance at variable switching frequency has been analyzed in MATLAB. The DC-link voltage is maintained at 380 V with a step input reference speed varying from 1200 rpm to 1500 rpm. Figure 3 shows the inverter voltage and current analysis at different inverter switching frequencies, while Figure 4 presents the PMSM motor speed response.

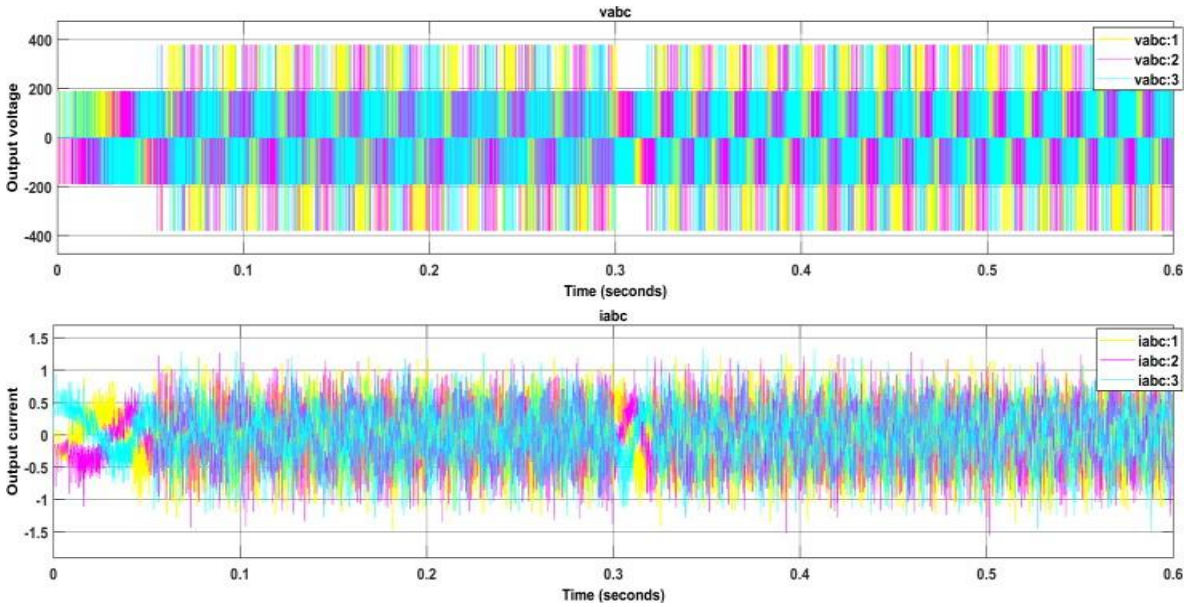

Figure 3. Inverter voltage and current analysis at constant inverter switching frequencies

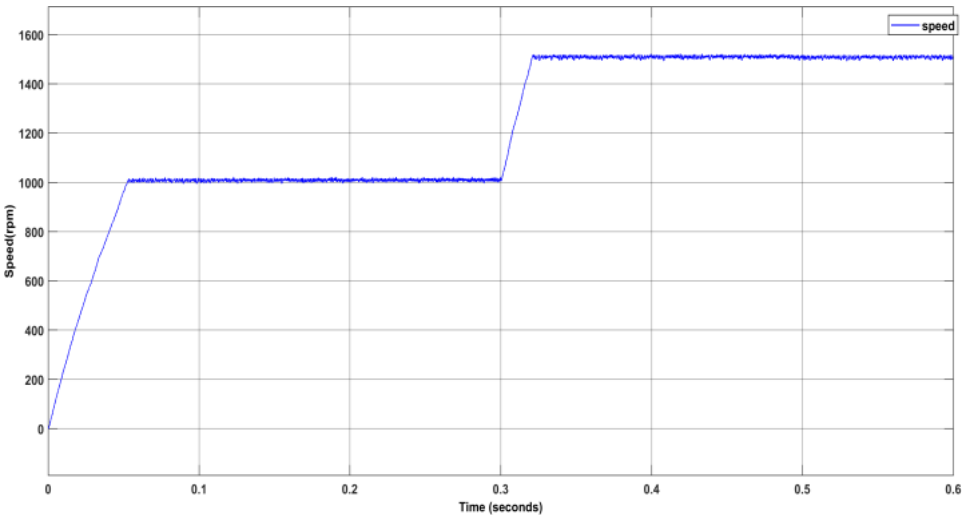

Figure 4. PMSM motor speed analysis

Figure 5 (in Appendix) presents the overall PMSM motor model analysis at 1500 rpm for the DTC-CBSVM PMSM drive operating under constant inverter switching frequency conditions. Figure 5(a) illustrates the motor torque analysis, showing the dynamic torque response and ripple characteristics. Figure 5(b) presents the stator current analysis of the PMSM drive. Figure 5(c) shows the stator voltage analysis under the same operating conditions. Similarly, Figures 6(a) to (c) (in Appendix) presents the PMSM motor model analysis at 1500 rpm for the FOC-CBSVM PMSM drive operating at constant inverter switching frequencies.

4.1. DTC–CBSVM PMSM drive analysis at constant inverter switching frequencies

This subsection presents the analysis of the DTC–CBSVM-controlled PMSM drive operating at constant inverter switching frequencies for EV applications. The purpose of this study is to evaluate the dynamic and steady-state performance of the proposed control strategy using a three-level twelve-switch NPC inverter fed PMSM drive. The analysis includes important performance parameters such as motor speed response, electromagnetic torque, stator current, stator voltage, switching frequency behavior, and harmonic performance under different operating conditions. The simulation is carried out in MATLAB/Simulink with a DC-link voltage of 380 V and reference speed variation from 1200 rpm to 1500 rpm to examine both transient and steady-state characteristics. The obtained results demonstrate that the DTC–CBSVM method provides improved torque response, reduced torque ripple, better voltage quality, and more controlled switching frequency characteristics, making it suitable for high-performance and efficient EV drive applications.

4.2. FOC–CBSVM PMSM drive analysis at constant inverter switching frequencies

This subsection presents the analysis of the FOC–CBSVM-controlled PMSM drive operating at constant inverter switching frequencies for EV applications. The purpose of this analysis is to evaluate the steady-state and dynamic performance of the proposed control strategy using a three-level twelve-switch NPC inverter fed PMSM drive. The study investigates important performance parameters such as motor speed response, electromagnetic torque, stator current, stator voltage, switching frequency characteristics, and harmonic performance under various operating conditions. The simulation is carried out in MATLAB/Simulink with a DC-link voltage of 380 V and reference speed variation from 1200 rpm to 1500 rpm to analyze both transient and steady-state responses of the drive system. The results demonstrate that the FOC–CBSVM method provides smooth speed control, reduced torque ripple, stable current characteristics, and fixed switching frequency operation, resulting in improved efficiency and reliable performance for EV drive applications.

4.3. Experimental model analysis

4.3.1. Direct torque control with carrier-based space vector modulation analysis

The hardware implementation of the proposed DTC–CBSVM PMSM drive consists of a 12 V power adapter, USB-to-UART bridge cable, TMEL motor control board, three-phase PMSM, and Atmel ATxmega16D4 processor board. The ATxmega16D4 provides sensorless DTC control using a back-EMF

phase-locked loop (PLL) for parameter tuning and motor control. Tables 1 and 2 present the comparative analysis of THD and torque ripple for DTC–NPCI and FOC–NPCI PMSM drives.

Table 1. Comparison of THD analysis

THD	DTC–NPCI PMSM (%)	FOC–NPCI PMSM (%)
Voltage	10.04	10.89
Current	2.33	2.41

Table 2. Torque ripple analysis

Controller speed (rpm)	DTC–NPCI PMSM (%)	FOC –NPCI PMSM (%)
1500	16.35	16.157

The results show that the proposed DTC–CBSVM method achieves lower harmonic distortion and reduced torque ripple, resulting in improved waveform quality and smoother motor operation. Figures 7(a) and (b) and 8(a) and (b) illustrate the voltage and current THD responses, confirming better harmonic performance of the proposed method. Figures 9 and 10 show the block schematic and experimental setup of the proposed twelve-switch NPCI PMSM drive.

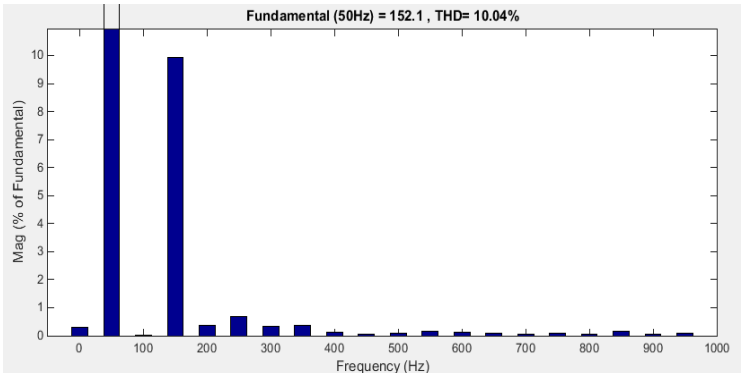

(a)

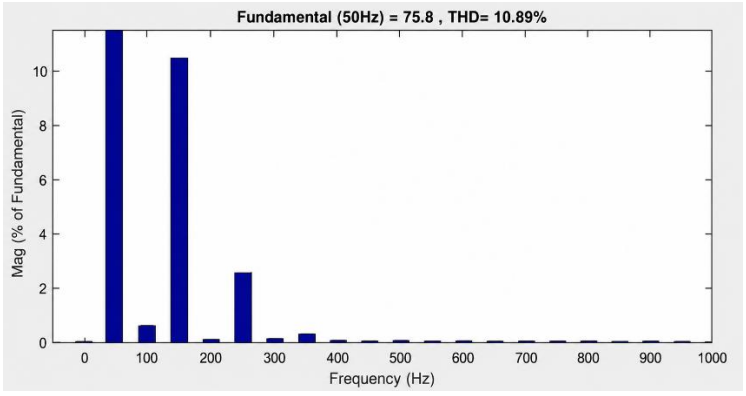

(b)

Figure 7. THD voltage response; (a) DTC–NPCI PMSM drive and (b) FOC –NPCI PMSM drive

Experimental results at 500 rpm, 1500 rpm, and 3000 rpm are presented in Figures 11–13, demonstrating stable speed tracking and good dynamic response over a wide operating range. Figures 14(a) and (b) and Tables 3–5 summarize the THD, motor speed, torque, current, DC-link voltage, and ripple analysis. The results indicate that as motor speed increases, motor current and torque decrease while the DC-link voltage remains constant, confirming efficient high-speed operation and improved drive performance for EV applications.

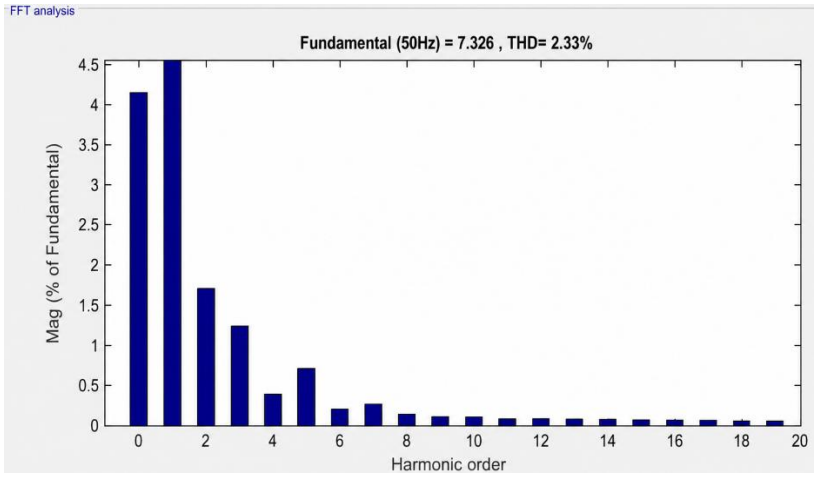

(a)

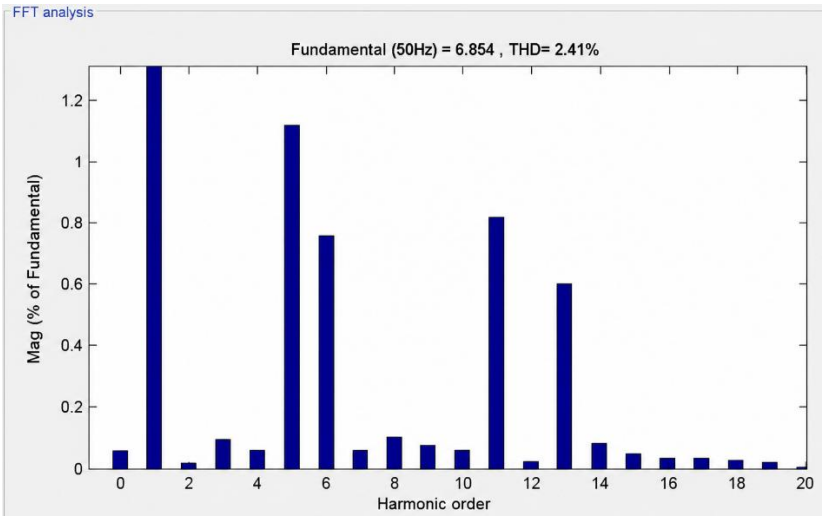

(b)

Figure 8. THD current response; (a) DTC–NPCI PMSM drive and (b) FOC–NPCI PMSM drive

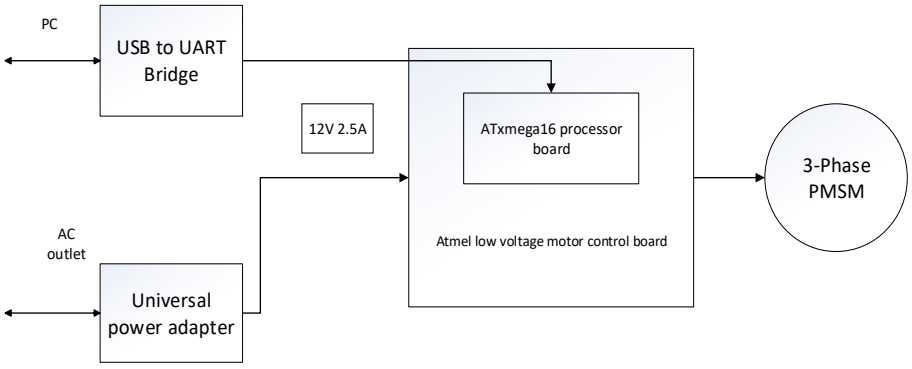

Figure 9. Block schematic of novel DTC-CBSVM twelve switch PCI PMSM drive

Figure 10. Experimental design of DTC-CBSVM twelve switch NPCI PMSM drive

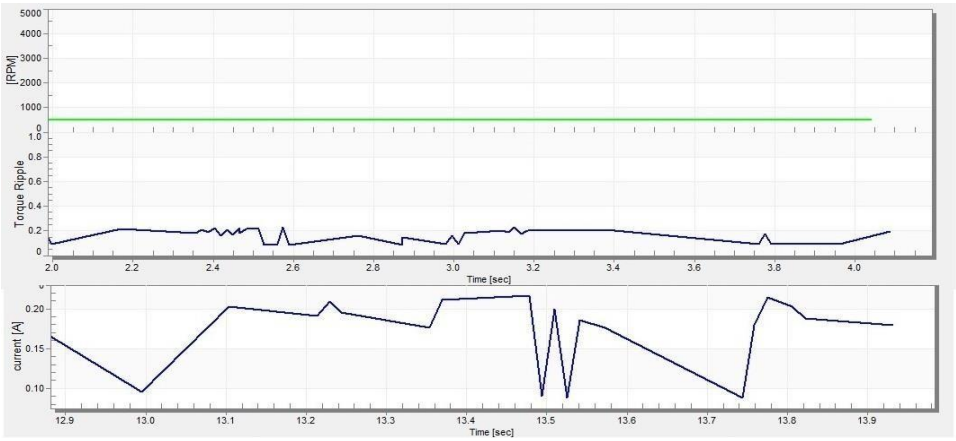

Figure 11. DTC-CBSVM twelve switch NPCI PMSM drive output at 500 rpm

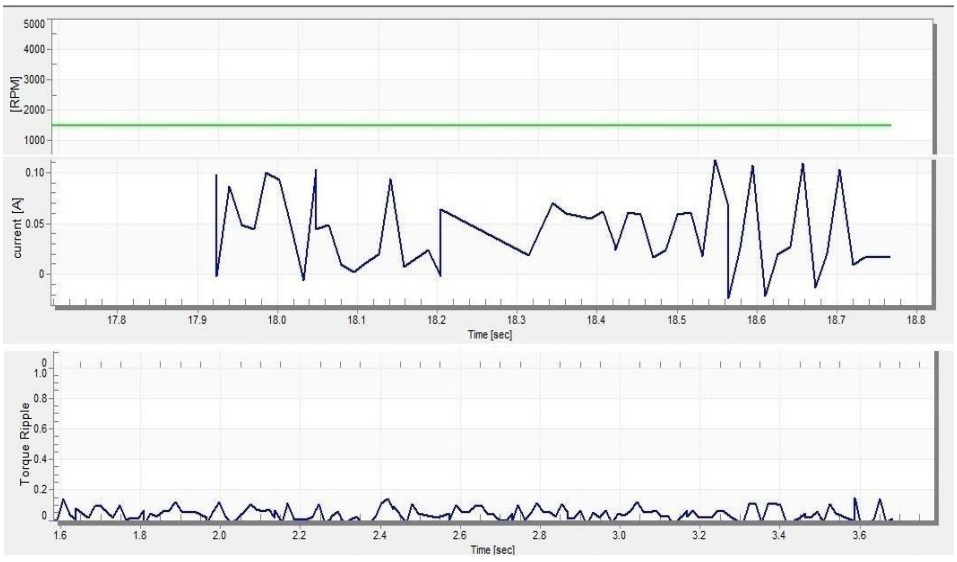

Figure 12. DTC-CBSVM twelve switch NPCI PMSM drive output at 1500 rpm

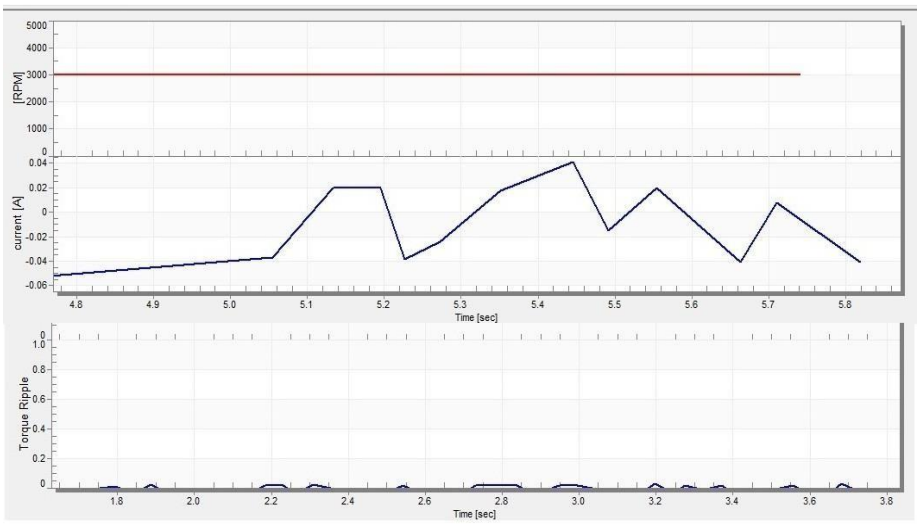

Figure 13. DTC-CBSVM twelve switch NPCI PMSM drive output at 3000 rpm

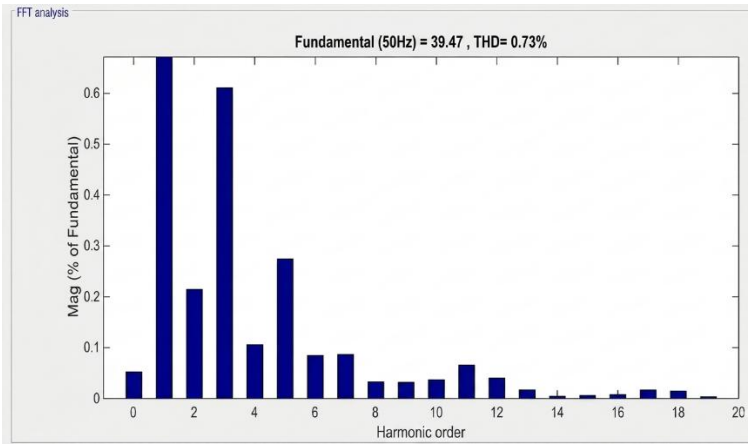

(a)

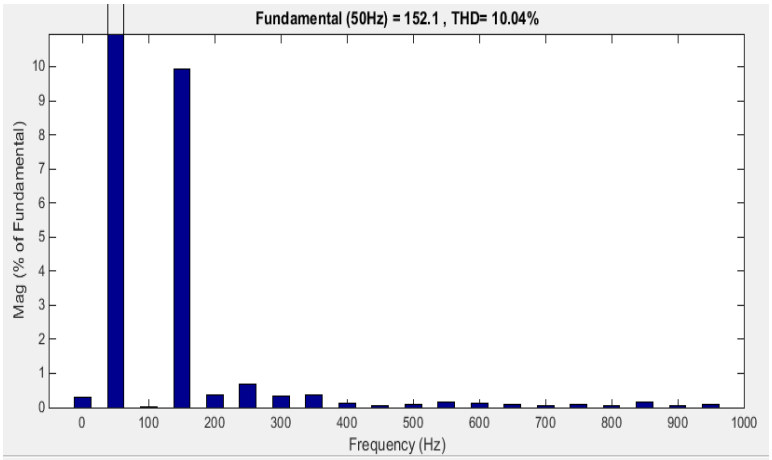

(b)

Figure 14.THD analysis of twelve switch NPCI; (a) voltage THD and (b) current THD

Table 3. Motor speed, torque current, and DC voltage variation

Motor speed (actual) (rpm)	Motor speed (measured) (rpm)	Motor current (actual) (A)	Motor current (measured) (A)	Motor direct voltage (actual) (V)	Motor torque ripple%
500	499.17	0.24	0.19	25.8	0.09
1500	1496.9	0.03	0.12	25.8	0.07
3000	3000	0.02	0.05	25.8	0.03

Table 4. THD analysis

Parameter	THD (%)
Voltage	10.04
Current	0.73

Table 5. Torque and current ripple analysis

FOC	1150 rpm	1250 rpm	1550 rpm
Motor torque	0.52 Nm	0.49 Nm	0.46 Nm
Motor current	8.4 mA	7.8 mA	7.5 mA

4.3.2. FOC–CBSVM analysis

The experimental setup of the proposed DTC–CBSVM PMSM drive consists of an AVR microcontroller, 4N35 optocoupler, FGA15N120AN IGBT drivers, and port B and port C interfacing circuits. Figure 15 shows the schematic diagram of the DTC–CBSVM PMSM drive, while Figure 16 presents the developed experimental hardware setup.

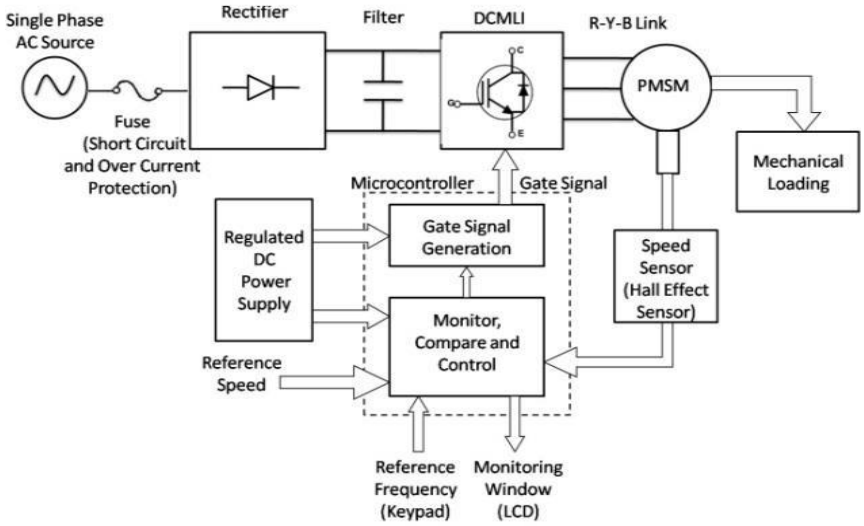

Figure 15. Schematic of FOC–CBSVM PMSM drive

The hardware output responses of the PMSM drive are shown in Figures 17 and 18 (in Appendix), validating the practical implementation of the proposed control strategy. Figure 17 shows the inverter line voltage responses for a resistive load at different operating frequencies. Figure 17(a) presents the line voltage response at 40 Hz, Figure 17(b) shows the response at 45 Hz, and Figure 17(c) illustrates the response at 50 Hz. The results demonstrate stable inverter voltage performance and improved waveform quality under varying frequency conditions.

Figure 18 shows the inverter phase voltage responses for an inductive load at different operating frequencies. Figure 18(a) presents the phase voltage response at 40 Hz, Figure 18(b) shows the response at 45 Hz, and Figure 18(c) illustrates the response at 50 Hz. The results indicate that the proposed DTC–CBSVM, method maintains stable voltage waveforms with improved output quality at different frequency conditions. Figure 19 presents the output current response of the DTC–CBSVM PMSM drive, which demonstrates smooth current characteristics with reduced ripple content.

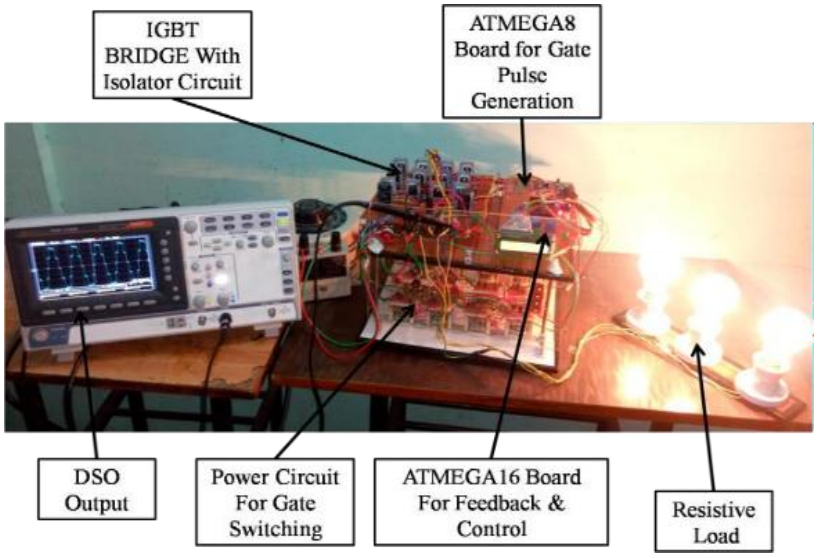

Figure 16. FOC–CBSVM experimental design

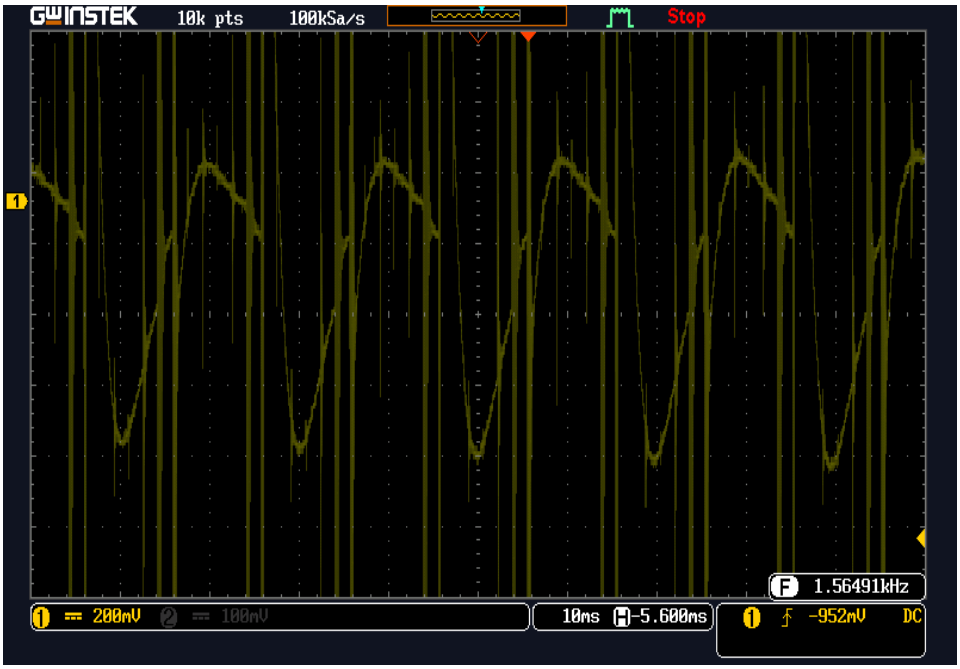

Figure 19. Output current response for motor FOC–CBSVM analysis

Figure 20 illustrates the load–speed variation at; 40 Hz (Figure 20(a)), 45 Hz (Figure 20(b)), and 50 Hz (Figure 20(c)), showing that the proposed drive maintains stable speed performance under varying load conditions. Figure 21 presents the torque versus load power characteristics, indicating improved torque capability and efficient power transfer at different operating frequencies.

Figure 22 shows the speed versus load power characteristics, confirming stable motor operation and better speed regulation as load changes. Figure 23 presents the speed versus torque characteristics, demonstrating that the proposed DTC–CBSVM method provides good torque production with stable speed response over a wide operating range. The obtained experimental results highlight the effectiveness of the proposed control strategy in reducing ripple, improving dynamic response, and enhancing the overall performance of PMSM drives for EV applications.

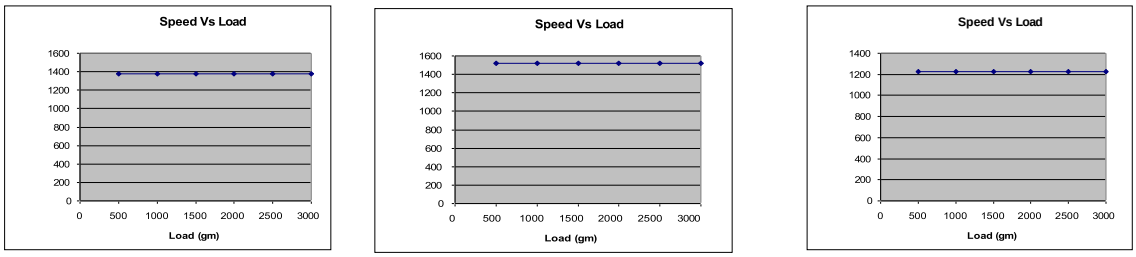

(a) (b) (c)

Figure 20. Load-speed variation at; (a) 40 Hz, (b) 45 Hz, and (c) 50 Hz

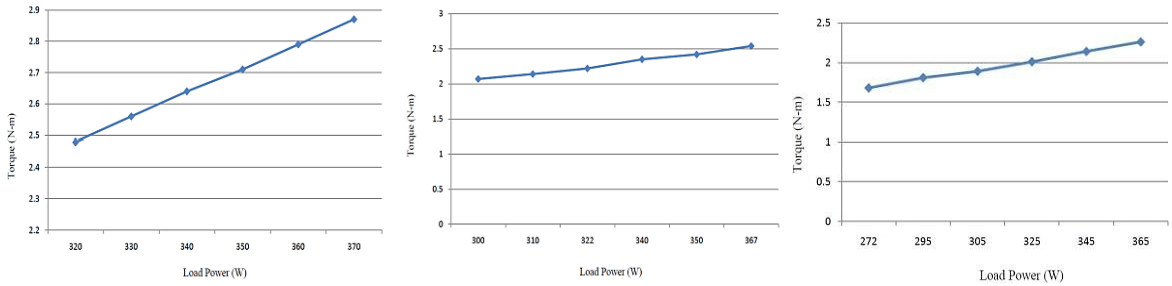

Figure 21. Torque versus load power characteristics at 40 Hz, 45 Hz, and 50 Hz

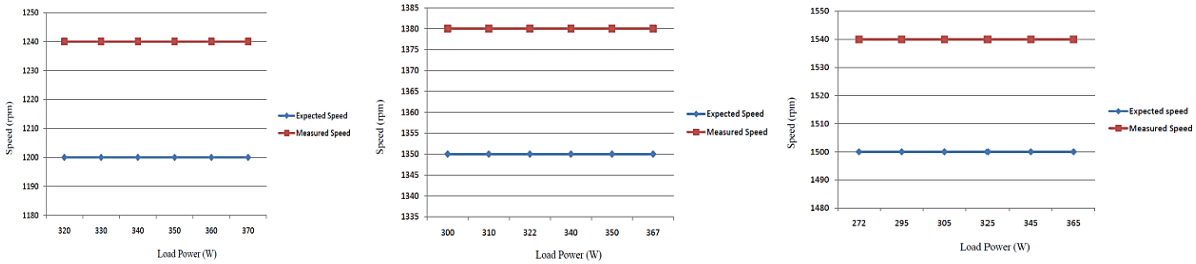

Figure 22. Speed versus load power characteristics at 40 Hz, 45 Hz, and 50 Hz

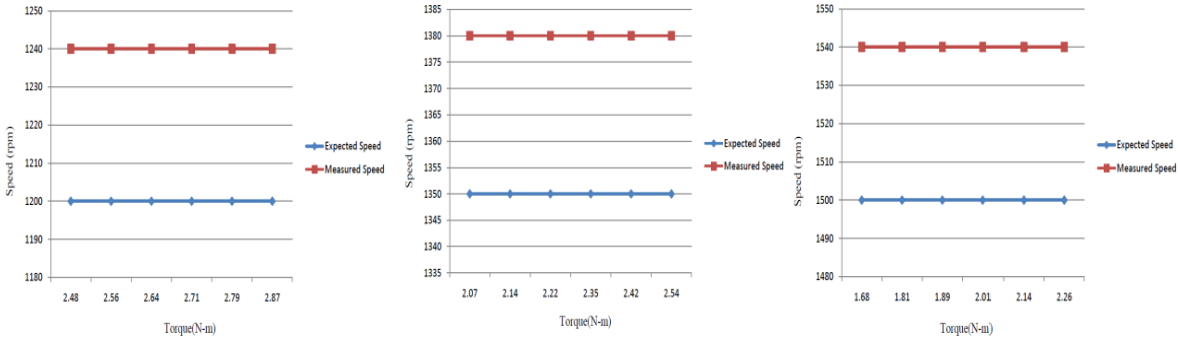

Figure 23. Speed versus torque characteristics at 40 Hz, 45 Hz, and 50 Hz

Table 6 shows speed variation with load at 40 Hz for motor and Table 7 shows speed variation with load at 45 Hz for motor. Table 8 shows variation in motor speed as a configuration of load at 50 Hz. The following are the hardware specification. Inverter DC link voltage=380 V, fundamental harmonic frequency fsw=50 Hz, switching frequency=2.5 kHz, and three-phase load power=1.5 KVA at unity power factor.

Table 6. Motor speed-load variation (40 Hz)

Weight	Voltage	Current	Power	Measured torque	Actual speed	Calculative speed
0.51	260	1.23	320	2.48	1200	1240
.2	260	1.26	330	2.56	1200	1240
1.5	260	1.3	340	2.64	1200	1240
2.5	260	1.34	350	2.71	1200	1240
2.7	260	1.38	360	2.79	1200	1240
3.5	260	1.42	370	2.87	1200	1240

Table 7. Motor speed-load variation (45 Hz)

Weight	Voltage	Current	Power	Measured torque	Actual speed	Calculative speed
0.51	264	1.13	300	2.08	1350	1380
1.2	264	1.13	300	2.08	1350	1380
1.5	264	1.17	310	2.15	1350	1380
2.5	264	1.21	320	2.22	1350	1380
2.7	264	1.25	330	2.29	1350	1380
3.5	264	1.25	330	2.29	1350	1380

Table 8. Motor speed-load variation (50 Hz)

Weight	Voltage	Current	Power	Measured torque	Actual speed	Calculative speed
0.51	270	1.03	280	1.78	1500	1540
1.2	270	1.11	300	1.91	1500	1540
1.5	270	1.14	310	1.97	1500	1540
2.5	270	1.22	330	2.1	1500	1540
2.7	270	1.29	350	2.22	1500	1540
3.5	270	1.37	370	2.35	1500	1540

Table 9 presents the variation in motor speed-load characteristics of the proposed DTC–CBSVM PMSM drive at 50 Hz. The results show that the supply voltage remains constant at 275 V, while the motor current, load power, and torque gradually increase with increasing load conditions. The torque increases from 1.7 Nm to 2.78 Nm as the load increases, indicating effective torque production and stable drive performance. The expected speed remains constant at 1510 rpm, while the measured speed is maintained at 1545 rpm under all loading conditions, demonstrating good speed regulation and stable dynamic response. These results confirm that the proposed DTC–CBSVM twelve-switch NPC inverter drive can maintain stable operation and efficient performance under varying load conditions, making it suitable for EV applications.

Table 9. Variation in motor speed-load (50 Hz)

Sr. No.	Load	Volt	Current	Load power	Torque	Expected speed	Measured speed
1	0.51	275	1.25	275	1.7	1510	1545
2	1.2	275	1.35	298	1.91	1510	1545
3	1.5	275	1.40	315	1.95	1510	1545
4	2.5	275	1.45	335	2.51	1510	1545
5	2.7	275	1.50	355	2.65	1510	1545
6	3.5	275	1.55	375	2.78	1510	1545

5. CONCLUSION

The comparative analysis of DTC-CBSVM and FOC for a PMSM fed by a three-level NPC inverter reveals that DTC-CBSVM provides faster torque response, reduced torque ripple, and improved dynamic performance, while FOC ensures stable switching frequency and higher steady-state efficiency. The three-level NPC inverter enhances both methods by minimizing THD and improving voltage utilization. Hence, DTC-CBSVM is ideal for dynamic EV operations, and FOC suits energy-efficient driving. Future research may focus on hybrid control strategies, intelligent optimization, and system integration to further enhance PMSM-based EV drive performance.

FUNDING INFORMATION

Authors state no funding involved.

AUTHOR CONTRIBUTIONS STATEMENT

This journal uses the Contributor Roles Taxonomy (CRediT) to recognize individual author contributions, reduce authorship disputes, and facilitate collaboration.

Name of Author	C	M	So	Va	Fo	I	R	D	O	E	Vi	Su	P	Fu
Rakesh Shriwastava	✓	✓	✓	✓	✓	✓	✓	✓	✓	✓	✓	✓	✓	✓
Balajee Maram	✓	✓		✓	✓	✓	✓		✓	✓		✓		✓
Yogesh S. Pawar	✓	✓	✓	✓	✓	✓		✓	✓	✓	✓			✓
Jyoti P. Rothe	✓	✓	✓		✓	✓	✓		✓	✓	✓	✓	✓	✓
Dinesh S. Wankhede	✓	✓		✓	✓	✓		✓	✓	✓			✓	
Hema Kale	✓	✓		✓	✓	✓		✓	✓	✓		✓	✓	✓

C : **C**onceptualization
M : **M**ethodology
So : **So**ftware
Va : **Va**lidation
Fo : **Fo**rmal analysis
I : **I**nvestigation
R : **R**esources
D : **D**ata Curation
O : Writing - **O**riginal Draft
E : Writing - Review & **E**diting
Vi : **Vi**sualization
Su : **Su**pervision
P : **P**roject administration
Fu : **Fu**nding acquisition

CONFLICT OF INTEREST STATEMENT

Authors state no conflict of interest.

DATA AVAILABILITY

The authors confirm that the data supporting the findings of this study are available within the article this study.

REFERENCES

[1] Takahashi and T. Noguchi, "A New Quick-Response and High-Efficiency Control Strategy of an Induction Motor," *IEEE Transactions on Industry Applications*, vol. IA-22, no. 5, pp. 820–827, 1986, doi: 10.1109/TIA.1986.4504799.

[2] J. Rodriguez, J. S. Lai, and F. Z. Peng, "Multilevel Inverters: A Survey of Topologies, Controls, and Applications," *IEEE Transactions on Industrial Electronics*, vol. 49, no. 4, pp. 724–738, 2002, doi: 10.1109/TIE.2002.801052.

[3] S. Kouro *et al.*, "Recent Advances and Industrial Applications of Multilevel Converters," *IEEE Transactions on Industrial Electronics*, vol. 57, no. 8, pp. 2553–2580, 2010, doi: 10.1109/TIE.2010.2049719.

[4] H. Akagi, "Multilevel Converters: Fundamental Circuits and Systems," in *Proceedings of the IEEE*, vol. 105, no. 11, pp. 2048–2065, 2017, doi: 10.1109/JPROC.2017.2682105.

[5] X. Wang, Z. Wang, M. Cheng, and Y. Hu, "Remedial Strategies of T-NPC Three-Level Asymmetric Six-Phase PMSM Drives Based on SVM-DTC," *IEEE Transactions on Industrial Electronics*, vol. 64, no. 9, pp. 6841–6853, 2017, doi: 10.1109/TIE.2017.2674591.

[6] K. B. Lee, J. H. Song, I. Choy, and J. Y. Yoo, "Torque Ripple Reduction in DTC of Induction Motor Driven by Three-Level Inverter With Low Switching Frequency," *IEEE Transactions on Power Electronics*, vol. 17, no. 2, pp. 255–264, 2002, doi: 10.1109/63.988674.

[7] D. Casadei, G. Serra, A. Tani, and L. Zarri, "Assessment of direct torque control for induction motor drives," *Bulletin of the Polish Academy of Sciences. Technical Sciences*, vol. 54, no. 3, pp. 237-254, 2006.

[8] T. Geyer and D. E. Quevedo, "Performance of Multistep Finite Control Set Model Predictive Control for Power Electronics," *IEEE Transactions on Power Electronics*, vol. 30, no. 3, pp. 1633–1644, 2015, doi: 10.1109/TPEL.2014.2316173.

[9] S. Xu, Z. Sun, C. Yao, H. Zhang, W. Hua, and G. Ma, "Model Predictive Control With Constant Switching Frequency for Three-Level T-Type Inverter-Fed PMSM Drives," *IEEE Transactions on Industrial Electronics*, vol. 69, no. 9, pp. 8839–8850, 2022, doi: 10.1109/TIE.2021.3114716.

[10] X. Tang and S. Niu, "Coherent Vector Based Model Predictive Control With Zero-Sequence Component Injection for Three-Level NPC Inverter Fed PMSM Drives," *IEEE Transactions on Power Electronics*, vol. 40, no. 10, pp. 14686–14696, 2025, doi: 10.1109/TPEL.2025.3578425.

[11] A. Madan and E. Bostancı, "Comparison of Two-Level and Three-Level NPC Inverter Topologies for a PMSM Drive for Electric Vehicle Applications," in *2019 International Aegean Conference on Electrical Machines and Power Electronics (ACEMP) & 2019 International Conference on Optimization of Electrical and Electronic Equipment (OPTIM)*, Istanbul, Turkey, 2019, pp. 147-154, doi: 10.1109/ACEMP-OPTIM44294.2019.9007197.

[12] K. K. Prabhakar, C. U. Reddy, A. K. Singh, and P. Kumar, "Inverter Switching Frequency Prediction in DTC of Induction Motor Drive for an EV Drivetrain," *IEEE PES General Meeting*, 2017, doi: 10.1109/PESGM.2017.8273912.

[13] M. Depenbrock, "Direct Self-Control (DSC) of Inverter-Fed Induction Machine," *IEEE Transactions on Power Electronics*, vol. 3, no. 4, pp. 420–429, 1988, doi: 10.1109/63.17963.

[14] J. Holtz, "Pulsewidth Modulation for Electronic Power Conversion," in *Proceedings of the IEEE*, vol. 82, no. 8, pp. 1194–1214, 1994, doi: 10.1109/5.301684.

[15] T. M. Jahns and W. L. Soong, "Pulsating Torque Minimization Techniques for Permanent Magnet AC Motor Drives," *IEEE Transactions on Industrial Electronics*, vol. 43, no. 2, pp. 321–330, 1996, doi: 10.1109/41.491356.

[16] C. Xia, Z. Li, and T. Shi, "A Control Strategy for Four-Switch Three-Phase Brushless DC Motor Using Single Current Sensor," *IEEE Transactions on Industrial Electronics*, vol. 56, no. 6, pp. 2058–2066, 2009, doi: 10.1109/TIE. 2009.2014307.
[17] Y. Korkmaz, F. Korkmaz, I. Topaloglu, and H. Mamur, "Comparing of Switching Frequency on Vector Controlled Asynchronous Motor," *International Journal of Soft Computing and Artificial Intelligence*, vol. 3, no. 4, pp. 9–16, 2015, doi: 10.15224/978-1-63248-081-1-66.
[18] N. Taib, T. Rekioua, and B. Francois, "An Improved Fixed Switching Frequency Direct Torque Control of Induction Motor Drives Fed by Direct Matrix Converter," *International Review of Electrical Engineering*, vol. 5, no. 2, pp. 620–628, 2010, doi: 10.1109/ISIE.2009.5218123.
[19] R. Krishnan, Permanent Magnet Synchronous and Brushless DC Motor Drives, CRC Press, 2010.
[20] B. K. Bose, Modern Power Electronics and AC Drives, Prentice Hall, 2002.
[21] P. Vas, Sensorless Vector and Direct Torque Control, Oxford University Press, 1998, doi: 10.1093/acprof:oso/9780198564652.001.0001
[22] H. Abu-Rub, A. Iqbal, and J. Guzinski, High Performance Control of AC Drives With MATLAB/Simulink Models, Wiley, 2012.
[23] M. P. Kazmierkowski and H. Tunia, Automatic Control of Converter-Fed Drives, Elsevier, 1994.
[24] R. Shriwastava, M. P. Thakre, K. V. Bhadane, M. S. Harne, and N. B. Wagh, "Performance enhancement of DCMLI fed DTC-PMSM drive in electric vehicle," *Bulletin of Electrical Engineering and Informatics*, vol. 11, no. 4, pp. 1867–1881, Aug. 2022, doi: 10.11591/eei.v11i4.3714.
[25] R. Shriwastava, S. Gosavi, S. S. Khule, S. Hadpe, and M. P. Thakre, "A novel PWM technique for reduced switch count multilevel inverter in renewable power applications," *International Journal of Applied Power Engineering*, vol. 12, no. 1, pp. 1–12, Mar. 2023, doi: 10.11591/ijape.v12.i1.pp1-12.

APPENDIX

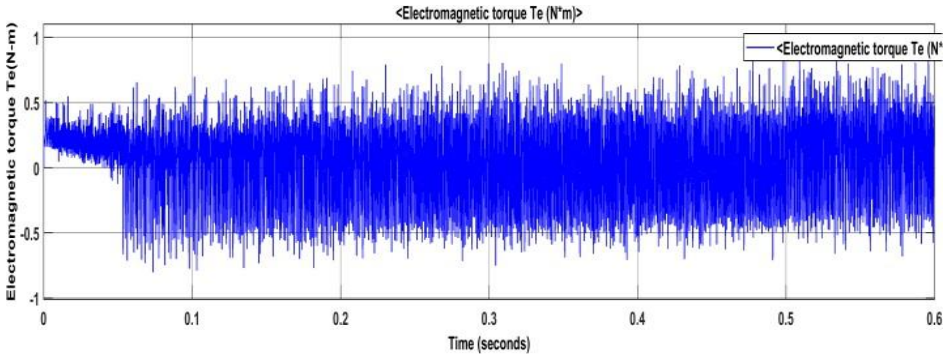

(a)

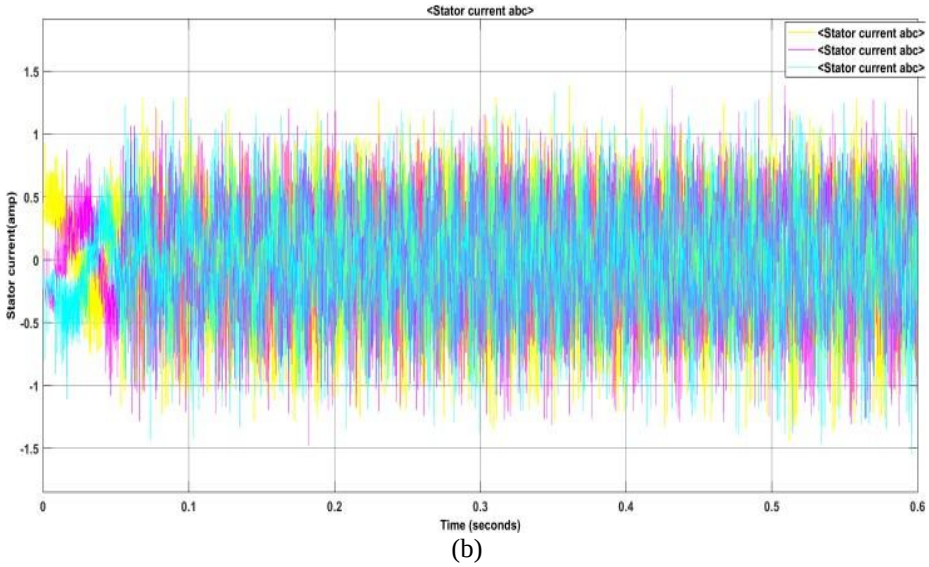

(b)

Figure 5. PMSM motor model analysis at 1500 rpm; (a) PMSM motor torque analysis and (b) PMSM motor stator currents analysis

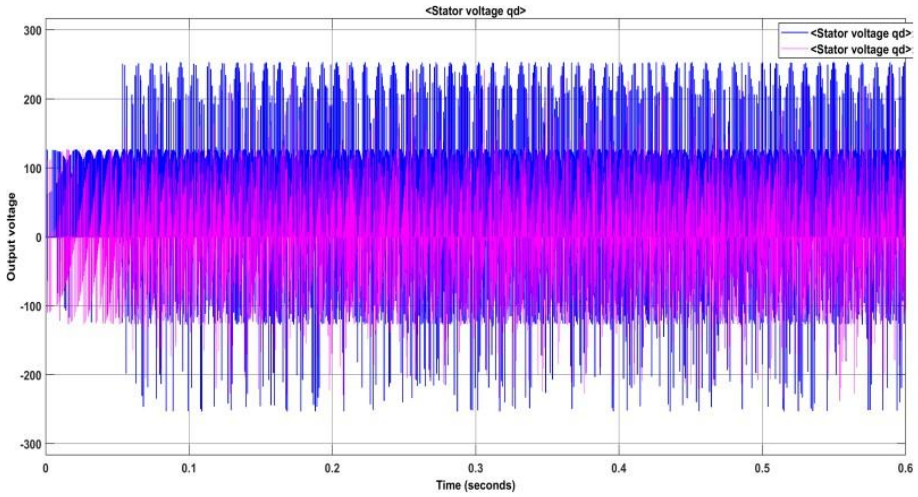

(c)

Figure 5. PMSM motor model analysis at 1500 rpm; (c) PMSM motor stator voltage analysis *(continued)*

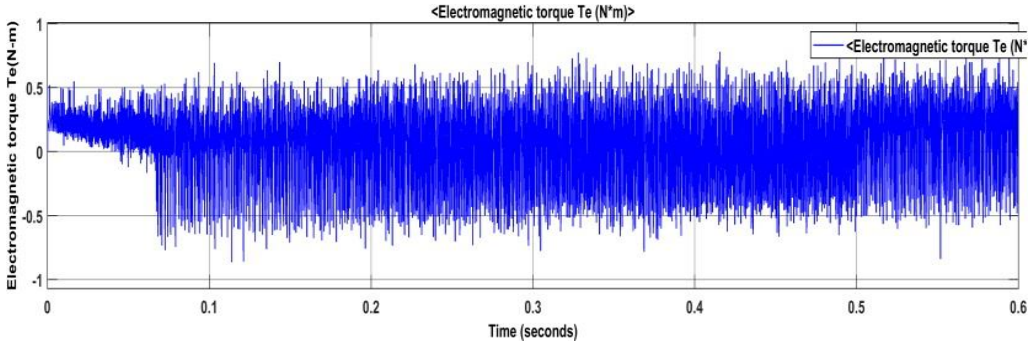

(a)

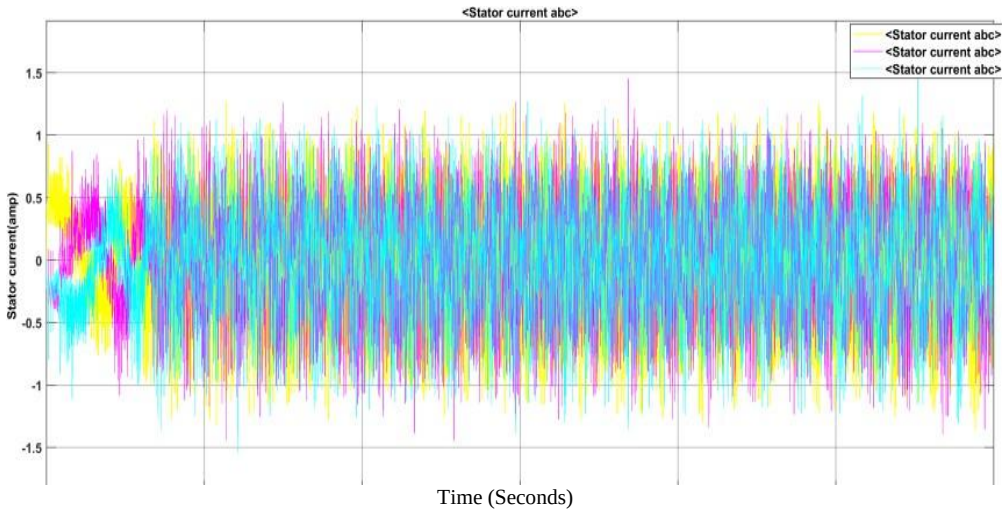

(b)

Figure 6. PMSM motor model analysis at 1500 rpm; (a) PMSM motor torque analysis and (b) PMSM motor currents analysis

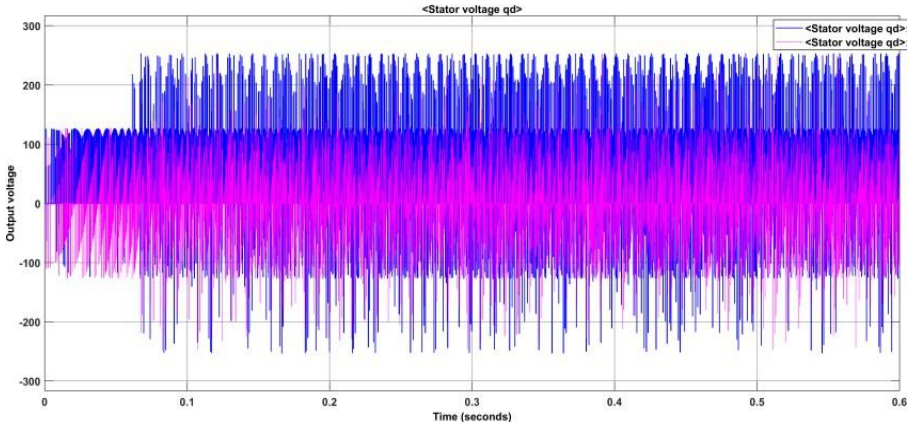

(c)

Figure 6. PMSM motor model analysis at 1500 rpm; (c) PMSM motor voltage analysis *(continued)*

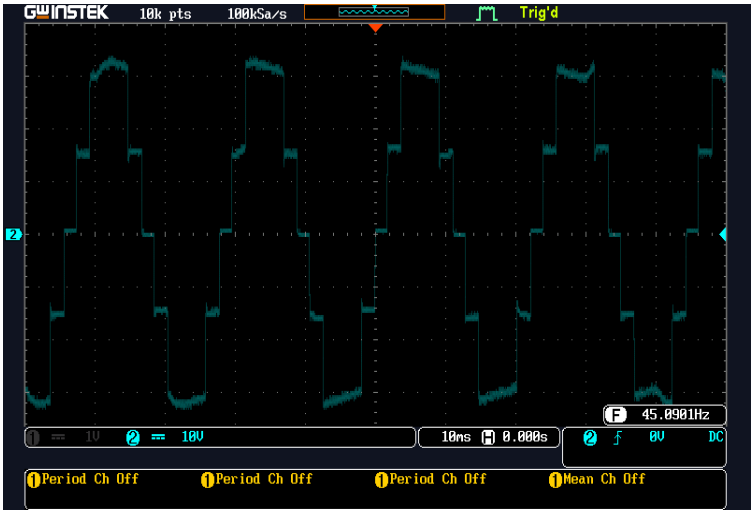

(a)

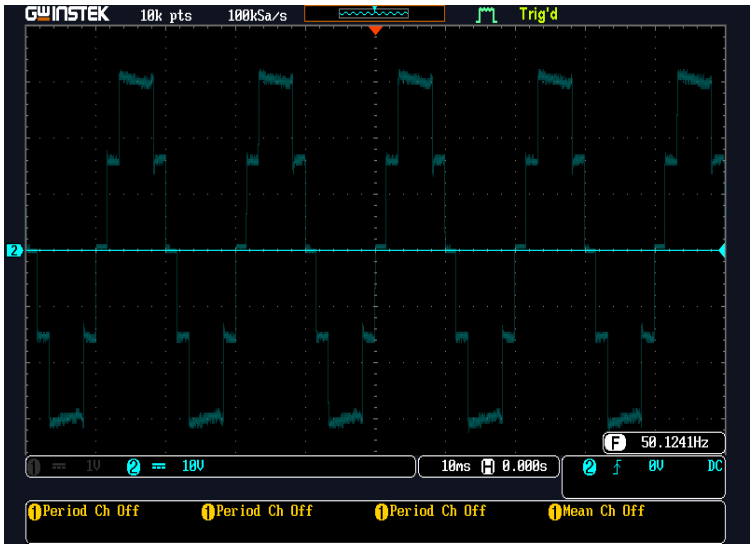

(b)

Figure 17. Inverter line voltages response of resistive load at; (a) 40 Hz and (b) 45 Hz

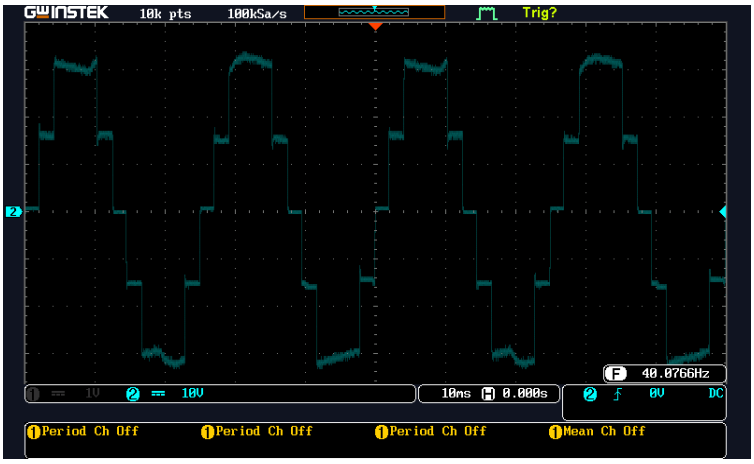

(c)

Figure 17. Inverter line voltages response of resistive load at; (c) 50 Hz *(continued)*

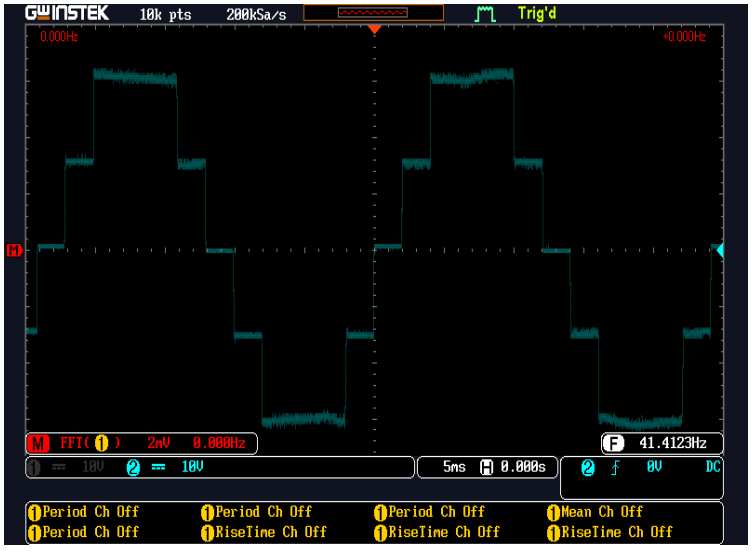

(a)

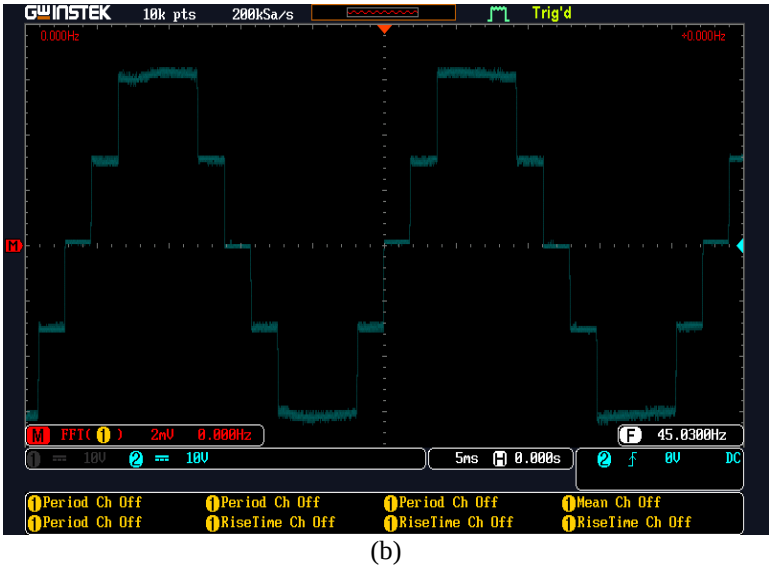

(b)

Figure 18. Inverter phase voltages response for inductive load at; (a) 40 Hz and (b) 45 Hz

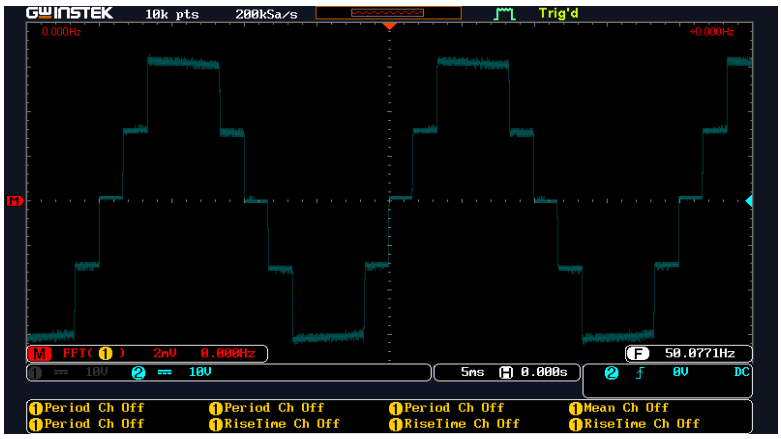

(c)

Figure 18. Inverter phase voltages response for inductive load at; (c) 50 Hz *(continued)*

BIOGRAPHIES OF AUTHORS

Dr. Rakesh Shriwastava obtained Ph.D. degree in electrical engineering specializing in power electronics and drives from RTM Nagpur University, (India) in 2017. He occupied various positions to serve the engineering institutes for about 24 years. He is currently working as Professor in the Department of Electrical Engineering, Govindrao Wanjari College of Engineering and Technology, Nagpur. His research interests include the analysis and control of electrical drives, particularly in hybrid and electric vehicle applications. He has several publications in national and international journals. He attended international and national conferences and also worked as a jury member. He is a member of professional bodies such as ISTE and IAENG. He can be contacted at email: rakesh_shriwastava@rediffmail.com.

Dr. Balajee Maram earned his Doctor of Philosophy (Ph.D.) from Bharathiar University, Coimbatore, Master Degree in Computer Science and Engineering from Anna University, Chennai, Master of Technology-Computer Science and Engineering from Swami Vivekanand University, Sagar, Madhya Pradesh, Bachelor of Technology-Computer Science from Himalayan University, Itanagar, Arunachal Pradesh, Master of Business Administration from Alagappa University, Karaikudi, M.A. (Master of Communication and Journalism) form Alagappa University, Karaikudi. He is currently working as a Professor in the Department of Computer Science and Engineering, Chandigarh University, Punjab. He has more than 18 years of teaching and research experience, 5 years of industry. He has 121 research publications in reputed journals which are indexed by SCIE and Scopus also. He has published 4 book-chapters in international publishers like Springer and IGI Global. He can be contacted at email: maram.balajee@gmail.com.

Dr. Yogesh S. Pawar received the B.E. degree in Electrical Engineering from Pune University, Nashik, PDVVPCOE, Ahmednagar, Maharashtra, India in 2010 and the M.Tech. degree in electrical power system from Mumbai University, Veermata Jijabai Technological Institute, Mumbai, Maharashtra, India, in 2012 and his Ph.D. degree from Bhabha University, Bhopal, Maharashtra, India in 2025. He is currently an Assistant Professor with the Department of Electrical Engineering, Loknete Gopinathaji Munde Institute of Engineering Education and Research, Nashik. He has over 13 years of teaching experience. His research interest includes power system, optimisation techniques, and artificial intelligence techniques. He is a life member of ISTE. He can be contacted at email: ysp.logmieer@gmail.com and yogesh.pawar@logmieer.edu.in.

Dr. Jyoti P. Rothe Completed B.E. in Electrical Engineering from Govt. College of Engineering, Amravati University, M.Tech. in Integrated Power System from VNIT, Nagpur and Ph.D. in Electrical Engineering from MITS, Gwalior, RGPV Bhopal. With 32 years of teaching experience, research interests are primarily in the area of electrical power system and power electronics. She can be contacted at email: rothejyoti04@gmail.com.

Dr. Dinesh S. Wankhede received the B.E. degree in Electrical Engineering from Amravati University, Amravati, SSGMCE, Shegaon, Maharashtra, India in 1999 and the M.E. degree in electrical power system from Shivaji University, Kolhapur, Walchand College of Engineering, Sangli, Maharashtra, India, in 2002 and his Ph.D. degree from Visvesvaraya National Institute of Technology, Nagpur, Maharashtra, India in 2019. He is currently an Associate Professor with the Department of Electrical Engineering, St. Vincent Pallotti College of Engineering and Technology, Nagpur. He has over 22 years of teaching experience. His research interest includes power electronics, optimization techniques, and artificial intelligence techniques. He is a Life Member of ISTE and recipient of the ISTE's L&T Best M.Tech. Thesis Award in 2001. He can be contacted at email: dineshhwankhede@gmail.com or dwankhede@stvincentngp.edu.in.

Dr. Hema Kale is a faculty member in the Department of Electronics and Telecommunication Engineering at St. Vincent Pallotti College of Engineering and Technology (SVPCET), Nagpur. She earned her Ph.D. from Nagpur University in 2015, M.Tech. in Electronics from YCCE, Nagpur in 2003, and B.E. in Electronics from Government College of Engineering, Amravati in 1993. She is the approved guide for Ph.D. She has over 25 years of teaching experience and 26 years of overall professional experience. She has published 12 papers in international journals, 10 papers in international conferences, and authored one book chapter. Her research interests include wireless communication, embedded systems, and signal processing. She holds multiple patents, including 2 granted patents on Subcarrier Allocation and Grouping (2021) & Embedded System based Expert System for Crop Harvesting Decisions (2026), along with published patents in agricultural expert systems and soil health monitoring. She has also registered copyrights for innovative MATLAB-based teaching tools. She is a recipient of the Outstanding Woman Researcher in Communication Engineering Award (VIWA 2021). She is the principal investigator of a funded research project titled "Design and Development of a Microcontroller-Based Electronic System for Chlorophyll Measurement and Plant Health Monitoring", sanctioned under the RTMNU University Research Project Scheme (URPS) with a grant of ₹3,00000 and has actively contributed to product development, industry-collaborative projects, and rural outreach through Unnat Bharat Abhiyan (UBA) activities. She can be contacted at email: hkale@stvincentngp.edu.in.